Journal of Materials Chemistry A

Accepted Manuscript

ROYAL SOCIETY OF CHEMISTRY

www.rsc.org/materialsA

Cite this: DOI: 10.1039/c0xx00000x

www.rsc.org/xxxxxx

ARTICLE TYPE

Electrochemical fabrication of carbon nanotube/polyaniline hydrogel film for all-solid-state flexible supercapacitor with high areal capacitance

Sha Zeng,[a,b] Hongyuan Chen,[a] Feng Cai,[a] Yirang Kang,[a] Minghai Chen,*[a] Qingwen Li*[a]

Received (in XXX, XXX) Xth XXXXXXXXX 20XX, Accepted Xth XXXXXXXXX 20XX
DOI: 10.1039/b000000x

Carbon nanotube (CNT) film is a favorable kind of substrate in flexible electric devices because of its superior flexibility, favorable mechanical strength and excellent electrical conductivity. Moreover, since conductive polymer polyaniline (PANI) owns high capacitance and easy manufacture method, it is always in favor for the supercapacitors. In this research, CNT film synthesized via floating catalyst chemical vapor deposition method could be further activated by electrochemically re-expanding to achieve better porosity and higher specific area, in order to obtain all-solid-state flexible supercapacitor with higher area capacitance. Comparing with the pristine CNT film characterized by PANI, electrochemically fabricated CNT hydrogel film with PANI deposition had higher specific area capacitance, which was 680 mF cm^{-2} at 1 mA cm^{-2}. All-solid-state supercapacitor that was synthesized by this composite film exhibited high specific area capacitance of 184.6 mF cm^{-2} at 1 mA cm^{-2}, which was higher than many similar supercapacitors. The rolling test showed that this supercapacitor maintained its high capacitance even in the rolling condition. After 500 charge-discharge cycles, it also remained high Coulombic efficiency and specific area capacitance. This all-solid-state supercapacitor shows great potential for energy storage device.

1. Introduction

Because of the increasing demand of the light, ultrathin, stretchable and portable electronic devices, flexible energy storage devices have attracted considerable interest.[1-6] Supercapacitor, which is also called electrochemical capacitors or ultracapacitor, combines the advantages of dielectric capacitor and rechargeable battery, thus can both deliver high power within a short time and store high amounts of energy.[7] Flexible portable supercapacitors require high areal capacitance for the aim of storing enough energy in limited space.[8] While general carbonous materials which store energy in their electrochemical double-layers have limited specific capacitance compared with pseudocapacitive materials.[9, 10, 11] Pseudocapacitive materials for supercapacitors, mainly containing several inorganic metal oxide compounds[12-14] and conductive polymers[15-19], usually exhibit much higher practical capacitance than carbonous materials, thus they have attracted much attention for the applications of flexible supercapacitor electrodes. However, inorganic pseudocapacitive materials usually have poor mechanical performance, therefore they could not be easily used for the electrodes of flexible supercapacitors with high capacitance. As a result, conductive polymers, including polyaniline (PANI),[20-22] polypyrrole (PPy)[23-25] and poly(3,4-ethylenedioxythiophene) (PEDOT),[26-28] have been widely investigated for flexible supercapacitors. Among these conductive polymers, PANI has best pseudocapacitive performance. However, its conductivity was still much lower than metallic current collectors for commercialized supercapacitors. A porous scaffold with large specific surface area and high conductivity was a key for the applications of PANI in flexible supercapacitors. Aqueous solution with sulphuric acid (H_2SO_4) was the best electrolyte for enlarging the pseudocapacitance of PANI, but most of the metallic current collectors which are usually used such as nickel (Ni) foam could be dissolved in this electrolyte. Porous carbons' scaffolds, such as carbon fiber cloth,[22] graphene [29-30] and carbon nanotube (CNT) film,[31] could be better for loading active materials as the electrodes of flexible supercapacitors. Among these scaffolds, the carbon fiber cloth could not exhibit high dispersion of PANI with high loading mass due to low specific surface area. Moreover, graphene film suffered from the closed pores formed by the restacking of graphene sheets. Different from these two scaffolds, CNT film was better for loading PANI because of its abundant open channels for electrolyte diffusion into the electrodes.

Although PANI can be dissolved in some organic solvents and then coated onto CNT film by immersing the latter into the former solutions, direct deposition is still an important strategy to obtain CNT films characterized with high loading mass of PANI.[32] The dense network and hydrophobic surface of CNT films largely affected the uniform deposition of PANI along the thickness direction of these films.[33] Usually in the electrodeposition process, PANI will firstly coat on the surface of CNT films and it could block the transmission and deposition of aniline molecules into the internal part of the film, especially for the films prepared via floating catalyst chemical vapor deposition (FCCVD) method which formed by thin CNTs (single-walled or double-walled CNTs) owning denser surface. Pulsed

electrodeposition strategy with tunable frequency can solve this problem to fabricate flexible CNT/conductive polymer composite film electrodes with conductive polymers uniform deposited in the whole film electrodes from top to bottom along, but the complicated process and low efficiency limited its applications, and the surface hydrophobic property was still not solved by this method. CNT sponges with much larger internal space than CNT films can easily achieve uniform deposition of conductive polymers, but their foam shape was largely different from film electrodes for common batteries. [34] If the dense CNT film can be expanded in a certain extent and surface activated, the deposition of PANI and other conductive polymers can be optimized.

In this research, cyclic voltammetry electrochemical oxidation process was used to activate high-performance CNT films prepared via floating catalyst chemical vapor deposition (FCCVD) methods. This activated CNT film symbolized as CNT hydrogel film was used for the electrodeposition of PANI to fabricate flexible composite film electrodes. This composite film symbolized as CNT/PANI hydrogel film showed more uniform distribution of PANI wrapping carbon nanotubes, meanwhile PANI did not cover the surface of the film. As a result, it exhibited higher areal capacitance than pristine CNT film/PANI composite film (CNT/PANI), which was 680 mF cm^{-2}. This high performance electrode was used to fabricate flexible symmetric supercapacitor with an areal capacitance up to 184.6 mF cm^{-2} which was much higher than most flexible supercapacitors. Furthermore, the specific capacitance remained stable after 500 cycles of charge-discharge and the Coulombic efficiency was almost as high as 100%.

2. Experimental Section

2.1 Materials

Carbon nanotube thin film was prepared by floating catalyst chemical vapor deposition (FCCVD) method followed by shrinking with ethanol. All other reagents were analytical grade, commercially available from Sinopharm Chemical Reagent Co. Ltd, and used without further purification.

2.2 Synthesis.

2.2.1 Fabrication of CNT hydrogel film

The pristine CNTs film was cut into same rectangular slices (1.5cm×4cm). Cu wires were embedded and connected to the CNT film with conductive Ag paste to form CNT film working electrode. A three-electrode system was used to achieve electrochemical activation of CNT film in 0.8 M H_2SO_4 aqueous solution. Graphite sheet was used for the counter electrode and saturated calomel electrode SCE was the reference electrode. Cyclic voltammetry (CV) strategy was applied in this system with the scan rate of 50 mV s^{-1} between 1 V and 2 V for 20 cycles in 0.8 M H_2SO_4 solution. In this process, CNT film was expanded in a certain extent (thickness from 0.01 mm to about 1.00 mm, and its surface was activated. After washing and drying processes, the electrochemically fabricated CNT hydrogel film was obtained.

2.2.2 Fabrication of CNT/PANI hydrogel film

The aqueous solution with aniline monomer (0.5 M) and H_2SO_4 (1 M) was used as the electrolyte for electrodepositing PANI onto CNT hydrogel films. Electrodeposition was carried out in a three-electrode system with a saturated calomel electrode (SCE) as the reference electrode, a Pt wire electrode as counter electrode and a piece of CNT hydrogel film as working electrode. Firstly, PANI was electrodeposited around the individual CNTs via cyclic voltammetry with the voltage of -0.2 V~0.8 V at the scan rate of 100 mV s^{-1}. The cyclic number was tuned from 200 to 500, with the aim of determining the most appropriate cyclic number. After the electrodeposition, the composite films were washed by deionized water and ethanol and dried in room temperature. Finally, the CNT/PANI hydrogel films were prepared.

2.2.3 Fabrication of flexible all-solid-state supercapacitor

Two pieces of identical activated CNT/PANI composite hydrogel film electrodes were prepared by lighting pressing activated CNT/films with Cu wires onto PET films. PVA-H_2SO_4 hydrogel electrolyte was prepared as follows: 1 g PVA powder and 10 mL deionized water were mixed and heated to 90°C under constant stirring until the solution became clear. After that, 1 g H_2SO_4 was added into the solution. The gel electrolyte was obtained after cooling the solution down. Appropriate amount of hydrogel electrolyte was smeared uniformly on the surface of CNT/PANI composite hydrogel film. The electrodes were dried in air at room temperature to vaporize the excess water. At last, the electrodes were stacked together face to face, forming a solid thin layer of PVA-H_2SO_4 electrolyte. As a result, after the packaging, CNT/PANI hydrogel supercapacitor device was obtained. The whole process was shown in Figure 1.

2.3 Materials Characterization.

The microstructure morphologies of the samples were investigated by field emission scanning electron microscopy (FE-SEM, Quanta 400 FEG, FEI), high resolution transmission electron microscopy (HRTEM, Tecnai G2 F20 S-Twin, FEI), and Raman spectrum (LabRAM HR Raman spectrometer, HORIBA Jobin Yvon).

2.4 Electrochemical Measurements.

Electrochemical performances experiments were carried out in CHI-660C electrochemical workstation and LANHE CT2001A electrochemical cell test equipment. The electrochemical performances of CNT/PANI hydrogel films of different cyclic number were investigated in 1 M H_2SO_4 aqueous solution.

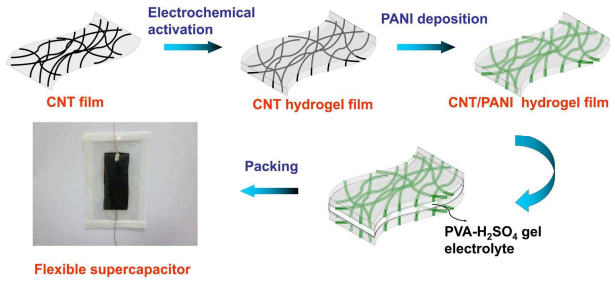

Figure 1 Stretch map of preparation process of CNT/PANI hydrogel flexible all-solid-state supercapacitor

3. Results and discussion

The surface morphology of pristine CNT film is shown in Figure S1, which indicates that this film was formed by CNT network with large bundles, individual CNTs and abundant open channels. In electrochemical activation process, each carbon nanotube acted as a microelectrode. In acid electrolyte, during the cyclic voltammetry process, hydrogen was produced on these

microelectrodes and then the hydrogen bubbles expanded the network of CNT film. Figure S2 shows the electrochemical performance of CNT film and CNT hydrogel film. Figure S3 indicates the electrochemical activation process enhanced the capacitance of CNT film significantly. Figure 2a and 2b show the SEM images of CNT/PANI composite films based on pristine and activated CNT films, respectively. Figure 2a reveals that PANI can be coated on individual CNTs and CNT bundles in the activated CNT film. This nanostructure largely benefit the uniform dispersion of PANI among the CNT network scaffold, thus its PANI utilization efficiency is relatively high. However, as shown in Figure 2b, the surface of pristine CNT film is fully coated by PANI layer, which covers most of the open channels in the CNT scaffold, thus blocks the diffusion of electrolytes into the electrode and reduces the utilizing efficiency of PANI as the electrochemical active materials. Figure 2c and 2d show the TEM images of the two samples, respectively. PANI layer is uniformly coated onto the surface of CNTs as shown in Figure 2c, in which PANI and CNT exhibit a uniform mixture. However, there are many PANI hollow nanospheres coated on the surface of on the pristine CNT film as shown in Figure 2d. By comparing CNT/PANI hydrogel and CNT/PANI, it indicated that the electrochemically re-expanding process helped increasing the practical specific area and promoting PANI to deposit around individual carbon nanotubes. The sketch map of forming process of these two samples was showed as Figure 2e.

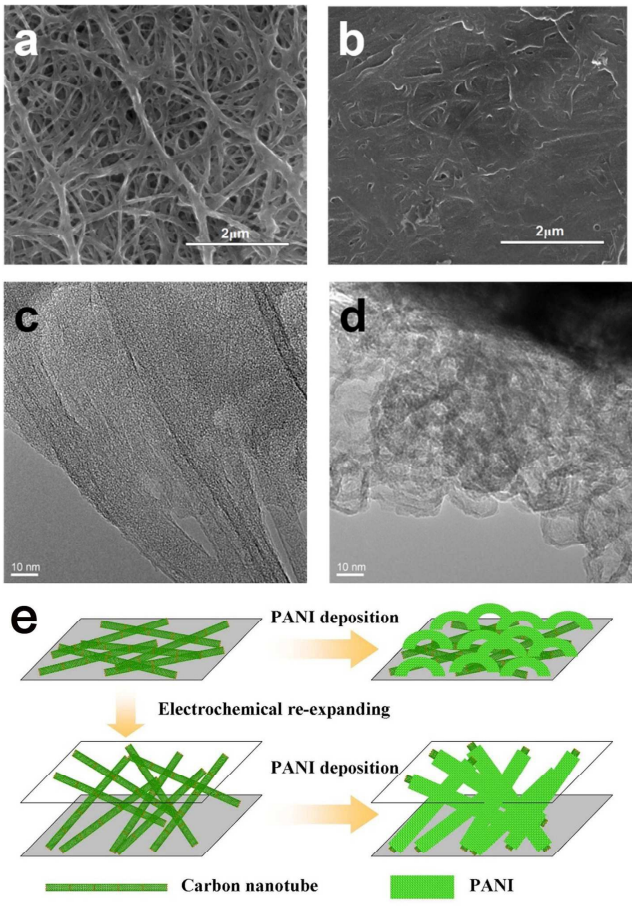

Figure 2 (a) SEM image of CNT/PANI hydrogel film; (b) SEM image of CNT/PANI film; (c) TEM image of CNT/PANI hydrogel film; (d) TEM image of CNT/PANI; (e) sketch map of forming process.

Figure 3 shows Raman spectra of pure pristine CNT film, CNT/PANI hydrogel film and CNT/PANI film. In the Raman spectra of pristine CNT film, the peak at 1331 cm^{-1} and 1583 cm^{-1} represent D band and G band of graphite crystal for carbon nanotube. The intensity ratio (I_D/I_G) of the pristine CNT film is 1.1, which indicates the medium crystallization of these CNTs, with conductive property and abundant surface defects. When PANI was electrodeposited onto CNT film, the peaks at 414 cm^{-1} and 574 cm^{-1} in Raman spectra of both CNT/PANI hydrogel film and CNT/PANI film is indicative of the C-N-C out-of-plane deformation mode and deformation mode of the protonated amine groups, respectively.[35] The peak at 809 cm^{-1} describes the C-H motion out of plane of PANI. Besides, the characteristic peaks at 1000-1700 cm^{-1} except for the D and G band are related to the PANI oxidation states. The presence of the bands at 1589 cm^{-1} (C–C deformation band of benzoid ring) and 1170 cm^{-1} (N–H bending deformation band of protonated amine) indicates that the PANI layer was fully oxidized.[36] After CV electrochemically re-expanding activation process, the carbon nanotubes were oxidized and decorated with oxygen-containing functional groups. The crystallization defective sites increased. As a result, in Figure 3, the intensity ratio (I_D/I_G) of CNT/PANI hydrogel film is larger than that of CNT/PANI film.[37]

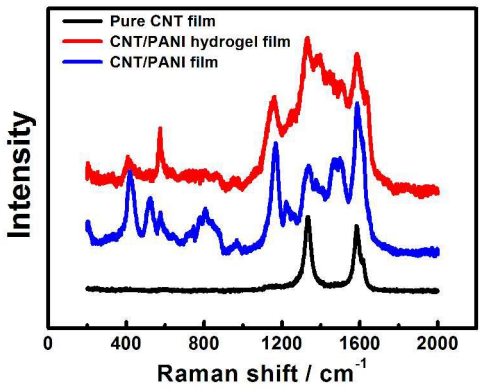

Figure 3 Raman spectra of pristine CNT film, CNT/PANI hydrogel film and CNT/PANI film

To determine the best deposition cycle number of PANI on activated CNT films, CNT/PANI hydrogel films were prepared via PANI deposition with different cyclic numbers. Figure 4a shows the electrochemical rate performance of different cycle numbers (200, 300, 400 and 500). It reveals that the practical capacitance of the composite films first increased and then decreased along with the increase of PANI electrodepositing cyclic numbers. The electrode material of CNT/PANI hydrogel with 400 cycles of PANI deposition exhibits better rate performance than other composite films. Further increasing the depositing cyclic number may reduce the practical surface area of the electrodes, thus decrease the utilization efficiency of PANI. As a result, the practical capacitance was decreased. Therefore, 400 is the appropriate value for PANI electrodeposition cycle number to prepare high-performance film electrodes. CV curves of this composite film at different scan rates (5, 10, 20, 40 mV s^{-1}) are shown in Figure 4b. Due to the processes of PANI redox transition, there are two pairs of redox peaks in the CV curves. At different scan rate, this CNT/PANI hydrogel film shows the

capacitive-like response in the whole potential range of investigation as showed. Figure 4c presents the charge-discharge curves at different current density (1, 2, 5, 8 and 10 mA cm^{-2}) within the same potential window (-0.2~0.7 V vs. SCE). The shape of charge-discharge curves is similar to faradic capacitors, which indicates that this film electrode is suitable for supercapacitors, and the charge or discharge curves are not straight lines, indicating the faradic processes. The capacitance of the CNT/PANI hydrogel film at 1 mA cm^{-2} is 0.68 F cm^{-2} that was much higher than many flexible electrodes such as carbonous films, conductive polymers and even metallic oxides. Figure 4d shows the specific capacitances of CNT/PANI hydrogel and CNT/PANI film electrode (with the same PANI deposition cycle number of 400). The electrochemical performance of CNT/PANI film is shown in Figure S4 in the supporting information. After calculating, the specific capacitance of CNT/PANI hydrogel film is 10%~25% higher than that of CNT/PANI film. The capacitance performance of CNT/PANI hydrogel film is better. The cyclic voltammetry re-expanding process results the uniform coating of PANI around the outer wall of individual CNTs and the formation of porous microstructure in CNT/PANI hydrogel film. This porous nanostructure simultaneously maintains the facile electrolyte penetration, fast proton exchange, and metallic conductivity, thus ensures highly electrochemical performance of the flexible film electrodes.

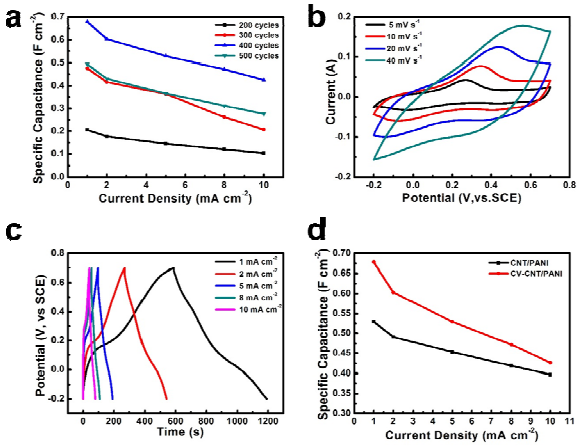

Figure 4 Electrochemical rate performance of CNT/PANI hydrogel film electrode with different deposition cycles (a); CV (b) and charge/discharge curves (c) of CNT/PANI hydrogel film with 400 cycles of deposition; rate performance comparison of CNT/PANI hydrogel film and CNT/PANI film with 400 cycles of deposition (d).

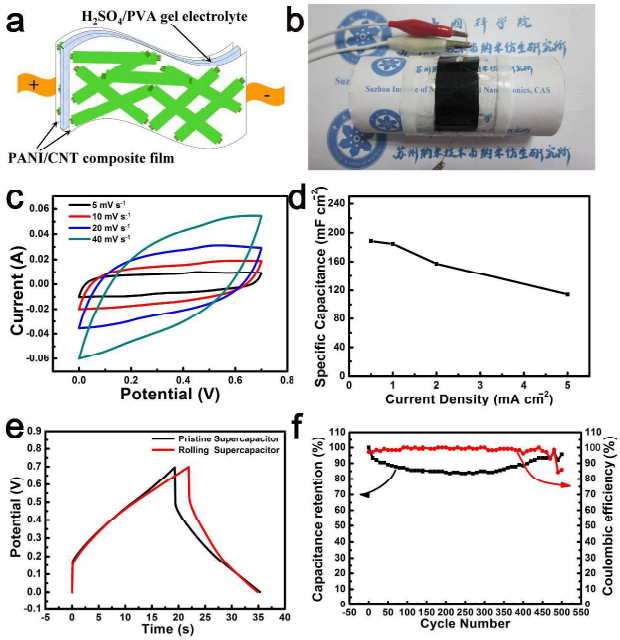

Figure 5 The sketch map (a) and optical image (b) of flexible supercapacitor based on CNT/PANI hydrogel film; CV curves (c) and rate performance (d) of flexible supercapacitor; the charge/discharge curves of the flexible supercapacitor at 5 mA cm^{-2} in planar and rolling condition (e); cyclic performance of the flexible supercapacitor (f).

As showed in Figure 5a, the sandwich structure of this all-solid-state flexible supercapacitor device is composed of two identical CNT/PANI hydrogel film electrodes and a layer of H_2SO_4/PVA gel electrolyte. PET thin films were used to package and protect the flexible supercapacitor. Figure 5b represents the optical image of this flexible supercapacitor. The electrochemical characterization of CNT/PANI hydrogel all-solid-state flexible supercapacitor was shown in Figure 5c~5f.

Table 1 Areal specific capacitance of different flexible electrode materials

Flexible electrode material	Areal capacitance for electrode (mF cm^{-2})	Areal capacitance for supercapacitor (mF cm^{-2})	Reference
Graphene/ cellulose paper	81	46	38
Active carbon cloth	88 (10 mV s^{-1})	-	39
Graphite nanosheets	-	2.3 (10 mA g^{-1})	40
RGO gel film	-	33.8 (1 mA cm^{-2})	41
Pure CNT	50 (1.4 mA cm^{-2})	-	42
RGO/ PANI	-	23	43
Graphite nanosheets/ PANI	355.6 (0.5 mA cm^{-2})	77.8	44
PEDOT/ cellulose	-	118	45
RGO/PPy	-	175	46
Graphene hydrogel-PANI/graphene	190.6(0.5 mA cm^{-2})	-	47
PPy/Paper	420 (1 mA cm^{-2})	-	48
Cellulose nanofiber /[PANI-RGO]	-	5.86 (0.0043 mA cm^{-2})	49
Cellulose nanofiber/[PANI-PEDOT]	-	4.22	49
SWCNT/ cellulose/ PANI	330	-	50
Graphite/ PEDOT/ MnO_2	316.4	-	51
CNT/PPy	280	-	42
$NiCo_2O_4$ nanowire	-	161 (1 mA cm^{-2})	52
CNT/TiO_2/ionomer	88 (5 mV s^{-1})	85 (5 mV s^{-1})	53
Fe_3O_4@SnO_2 core-shell nanorod array	7.013 (0.2 mA cm^{-2})	-	54
Fe_2O_3 nanorod array/carbon cloth	382.7 (0.5 mA cm^{-2})	-	55
CNT/PANI hydrogel film	680 (1 mA cm^{-2})	184.6 (1 mA cm^{-2})	This work

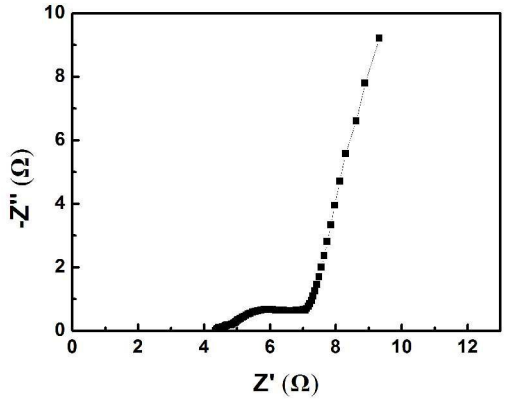

Figure 6. Nyquist plot (100 kHz-10 mHz) of CNT/PANI hydrogel all-solid-state flexible supercapacitor

As shown in Figure 5c, CV curves of the flexible supercapacitor exhibit typical rectangular shape approximately, suggesting that it's similar to EDL supercapacitor, which is an ideal supercapacitor in applications. It can be seen that the shape is almost maintained along with the increase of scan rate. Charge-discharge curves of the flexible supercapacitor at different current density are showed in Figure S5. The charge and discharge curves are straight lines and symmetrical to each other, suggesting the non-faradic processes and high Coulombic efficiency. Figure 5d shows the rate performance of this device. C_{sp} of the capacitor at 1 mA cm^{-2} is 184.6 mF cm^{-2}. Comparing with different flexible supercapacitor materials, the specific capacitance of electrode and supercapacitor device are much higher, as shown in Table 1.[38-55] Even at a current density up to 5 mA cm^{-2}, the C_{sp} of this device can retain a high value of 120 mF cm^{-2}, which indicates that the good rate performance of this supercapacitor device. In order to investigate whether this device can be operated in rolling condition, we tested the charge-discharge performance of it in rolling condition just as shown in Figure 5b. The result of Figure 5e demonstrates that the charge-discharge curve of rolling supercapacitor is similar to that of pristine condition at 5 mA cm^{-2} and the C_{sp} values are almost the same. As a result, the CNT/PANI hydrogel all-solid-state flexible supercapacitor can be available in rolling or bending condition. Furthermore, the cyclic performance of the flexible supercapacitor was investigated with the charge-discharge current density of 1 mA cm^{-2} as shown in Figure 5f. The capacitance of the flexible supercapacitor remained almost the same after 500 cycles of charge-discharge. During long time charge-discharge cycles, the utilization factor of the electrochemically active material might decrease, therefore the capacitance decreased until 300 cycles. While, the electrolyte of the CNT/PANI hydrogel flexible supercapacitor was gel electrolyte. After long time of charge-discharge cycles, the gel electrolyte penetrated into the inner layers and contacted with the unutilized active materials. The capacitance increased slightly after 300 cycles.[56] Overall, the cyclic performance was still very good for supercapacitors. Also, the Coulombic efficiency remained almost 100%. In Figure 6, the Nyquist plot of the flexible supercapacitor was tested in the open circuit potential of 0.013 V and amplitude of 5 mV. The Nyquist plots shows the electrolyte resistance of the CNT/PANI hydrogel flexible supercapacitor is about 4.3 Ω and the charge-transfer resistance of is about 1.5 Ω. The result suggests that the fast charge transfer process in the CNT/PANI all-solid-state flexible supercapacitor.

4. Conclusions

We have fabricated all-solid-state flexible supercapacitor via electrochemically activating the FCCVD CNT film and then electrochemically decorating PANI around individual CNT/CNT bundles. Electrochemically activating process increased the internal space of the dense CNT film to promote the decoration of PANI, thus increased the electrochemical performance. The supercapacitor based on the CNT/PANI hydrogel film exhibited high areal capacitance, good flexibility, and long cycle lifetime, thus could be promising for high-performance flexible energy storage devices.

Acknowledgement

The project was supported by the National Science Foundation of China (No.21203238), the National Basic Research Program (No.2010CB934700), and Production and Research Collaborative Innovation Project of Jiangsu Province, China (No. BY2011178).

Notes and references

[a]*Division of Advanced Nanomaterials and Key Lab of Nanodevices and Applications, Suzhou Institute of Nano-Tech and Nano-Bionics, Chinese Academy of Sciences, Suzhou 215123, PR China; Tel: 0512-62872803; E-mail: mhchen2008@sinano.ac.cn*

[b]*University of Chinese Academy of Sciences, Beijing 100049, PR China*

1 H. J. Lin, L. Li, J. Ren, Z. B. Cai, L. B. Qiu, Z. B. Yang and H. S. Peng, *Sci. Rep.*, 2013, **3**, 1353-1358.
2 T. Chen, H. S. Peng, M. Durstock and L. M. Dai, *Sci. Rep.*, 2014, **4**, 3612-3618.
3 Z. B. Yang, J. Deng, X. L. Chen, J. Ren and H. S. Peng, *Angew. Chem. Int. Ed.*, 2013, **52**, 13453–13457.
4 X. M. Lu and Y. N. Xia, *Nat. Nanotech.*, 2006, **1**, 163-164.
5 J. R. Miller, *Science*, 2012, **335**, 1312-1313.
6 M. H. Yu, Y. F. Zhang, Y. X. Zeng, M. S. Balogum, K. C. Mai, Z. S. Zhang, X. H. Lu and Y. X. Tong, *Adv. Mater.*, 2014, **26**, 4724–4729.
7 P. Simon and Y. Gogotsi, *Nat. Mater.*, 2008, **7**, 845-854.
8 D. W. Wang, F. Li, J. P. Zhao, W. C. Ren, Z. G. Chen, J. Tan, Z. S. Wu, I. Gentle, G. Q. Lu and H. M. Cheng, *ACS Nano*, 2009, **3**, 1745-1752.
9 G. P. Wang, L. Zhang and J. J. Zhang, *Chem. Soc. Rev.*, 2012, **41**, 797–828.
10 D. Y. Qu, J. *Power Sources*, 2002, **109**, 403-411.
11 G. Y. Yu, W. X. Chen, Y. F. Zheng, J. Zhao, X. Li and Z. D. Xu, *Mater. Lett.*, 2006, **60**, 2453-2456.
12 M. S. Wu and P. C. Chiang, *Electrochem. Solid-State Lett.*, 2004, **7**, A123-A126.
13 W. Sugimoto, H. Iwata, Y. Murakami and Y. Takasu, *J. Electrochem. Soc.*, 2004, **151**, A1181-A1187.
14 X. P. Dong, W. H. Shen, J. L. Gu, L. M. Xiong, Y. F. Zhu, H. Li and J. L. Shi, *J. Phys. Chem. B*, 2006, **110**, 6015-6019.
15 K.R. Prasad, K. Koga and N. Miura, *Chem.Mater.*, 2004, **16**, 1845-1847.
16 M. Kalaji, P. J. Murphy and G. O. Williams, *Synth. Met.*, 1999, **102**, 1360-1361.
17 Y. K. Zhou, B. L. He, W. J. Zhou, J. Huang, X. H. Li, B. Wu and H. L. Li, *Electrochim. Acta*, 2004, **49**, 257-262.
18 V. Gupta and N. Miura, *Mater. Lett.*, 2006, **60**, 1466-1469.
19 L. Z. Fan and J. Maier, *Electrochem. Commun.*, 2006, **8**, 937-940.
20 Q. Wu, Y. X. Xi, Z. Y. Yao, A. R. Liu and G. Q. Shi, *ACS. Nano*, 2010, **4**, 1963-1701.

21 C. Z. Meng, C. H. Liu, L. Z. Chen, C. H. Hu and S. S. Fan, *Nano Lett.*, 2010, **10**, 4025-4031.

22 M. Zhong, Y. Song, Y. F. Li, C. Ma, X. L. Zhai, J. L. Shi, Q. G. Guo and L. Liu, *J. Power Sources*, 2012, **217**, 6-12.

23 B. C. Kim, C. O. Too, J. S. Kown, J. M. Bo and G. G. Wallace, *Synthetic Materials*, 2011, **161**, 1130-1132.

24 Y. Shi, L. J, B. R. Liu, Y. Q. Wang, Y. Cui. Z. N. Bao and G. H. Yu, *J. Mater. Chem. A*, 2014, **2**, 6086-6091.

25 X. T. Ding, Y. Zhao, C. G. Hu, Y. Hu, Z. L. Dong, N. Chen, Z. P. Zhang and L. T. Qu, *J. Mater. Chem. A*, **2**, 12355-12360.

26 A. Laforgue, *J. Power Sources*, 2011, **196**, 559-564.

27 B. Anthumakkool, R. Soni, S. N. Bhange and S. Kurungot, *Energ. Environ. Sci.*, 2015, **8**, 1339-1347.

28 Y. B. Xie, H. X. Du and C. Xia, *Microporous Mesoporous Mater.*, 2015, **204**, 163-172.

29 K. Chi, Z. Y. Zhang, J. B. Xi, Y. A. Huang, F. Xiao, S. Wang and Y. Q. Liu, *ACS. Appl. Mater. Inter.*, 2014, **6**, 16312-16319.

30 M. H. Yu, Y. C. Huang, C. Li, Y. X. Zeng, W. Wang, Y. Li, P. P. Fang, X. H. Lu and Y. X .Tong, *Adv. Funct. Mater.*, 2015, **25**, 324–330.

31 C. Z. Meng, C. H. Liu, L. Z. Chen, C. H. Hu and S. S. Fan, *Nano Lett.*, 2010, **10**, 4025–4031.

32 X. L. Chen, H. J. Lin, P. N. Chen, G. Z. Guan, J. Deng and H. S. Peng. *Adv. Mater.*, 2014, **26**, 4444–4449.

33 J. L. Liu, J. Sun and L. Gao, *J. Phys. Chem. C,* 2010, **114***,* 19614–19620.

34 M. H. Yu, W. T. Qiu, F. X. Wang, T. Zhai, P. P. Fang, X. H. Lu and Y. X. Tong, *J. Mater. Chem. A*, 2015, **3**, 15792–15823.

35 M. Tagowska, B. Palys and K. Jackowska, *Synth. Met.*, 2004, **142**, 223-229.

36 J.Benson, I. Kovalenko, S. Boukhalfa, D. Lashmore, M. Sanghadasa and G. Yushin, *Adv. Mater.*, 2013, **25**, 6625-6632.

37 B.W. Kim, H. Chung and W. Kim, *J. Phys. Chem. C*, 2010, **114**, 15223-15227.

38 Z. Weng, Y. Su, D. W. Wang, F. Li, J. H. Du and H. M. Cheng, *Adv. Energy. Mater.*, 2011, **1**, 917-922.

39 G. M. Wang, H. Y. Wang, X. H. Lu, Y. C. Ling, M. H. Yu, T. Zhai, Y. X. Tong and Y. Li, *Adv. Mater.*, 2014, **26**, 2676-2682.

40 G.Y. Zheng, L. B. Hu, H. Wu, X. Xie and Y. Cui, *Energy Environ. Sci.*, 2011, **4**, 3368-3373.

41 U. N. Maiti, J. Lim, K. E. Lee, W. J. Lee and S. O. Kim, *Adv. Mater.*, 2014, **26**, 615-619.

42 Y. L. Chen, L. H. Du, P. H. Yang, P. Sun, X. Yu and W. J. Mai, *J. Power Sources*,2015, **287**, 68-74.

43 X. B. Zang, X. Li, M. Zhu, X. M. Li, Z. Zhen, Y. J. He, K. L. Wang, J. Q. Wei, F. Y. Kang and H. W. Zhu, *Nanoscale*, 2015, **7**, 7318-7322.

44 B. Yao, L. Y. Yuan, X. Xiao, J. Zhang, Y. Y. Qi, J. Zhou, J. Zhou, B. Hu and W. Chen, *Nano Energy*, 2013, **2**, 1071-1078.

45 B. Anothumakkool, R. Soni, S.N. Bhange and S. Kurungot, *Energy Environ. Sci.*, 2015, **8**, 1339-1347.

46 J. T. Zhang, P. Chen, B. H. L. Oh and M. B. Chan-Park, *Nanoscale*, 2013, **5**, 9860-9866.

47 K. Chi, Z. Y. Zhang, J. B. Xi, Y. A. Huang, F. Xiao, S. Wang and Y. Q. Liu, *ACS Appl. Mater. Inter.*, 2014, **6**, 16312–16319.

48 L. Y. Yuan, B. Yao, B. Hu, K. F. Huo, W. Chen and J Zhou, *Energy. Environ. Sci.*, 2013, **6**, 470-476.

49 X. Wang, K. Z. Gao, Z.Q. Shao, X. Q. Peng, X. Wu and F. J. Wang, *J. Power Sources*, 2014, **249**, 148-155.

50 D. T. Ge, L. L. Yang, L. Fan, C. F. Zhang, X. Xiao and Y. Gogotsi, *Nano Energy*, 2014, **11**, 568-578.

51 P. Y. Tang, L. J. Han and L. Zhang, *ACS Appl. Mater. Inter.*, 2014, **6**, 10506-10515.

52 Q. F. Wang, X. F. Wang, B. Liu, G. Yu, X. J. Hou, D. Chen and G. Z. Shen, *J. Mater. Chem. A*, 2013, **1**, 2468-2473.

53 C. Huang, N. P. Younga and P. S. Granta, *J. Mater. Chem. A*, 2014, **2**, 11022-11028.

54 R. Z. Li, X. Ren, F. Zhang, C. Du and J. P. Liu, Chem. Commun. 2012, **48**, 5010-5012.

55 X. H. Lu, Y. X. Zeng, M. H. Yu, T. Zhai, C. L. Liang, S. L. Xie, M. S. Balogun and Y. X. Tong, A*dv. Mater.*, 2014, **26**, 3148-3155.

56 S. W. Pan, H. J. Lin, J. Deng, P. N. Chen, X. L. Chen, Z. B. Yang and H. S. Peng. *Adv. Energy Mater.*, 2015, **5**, 1401438-1401444.

Table of Contents

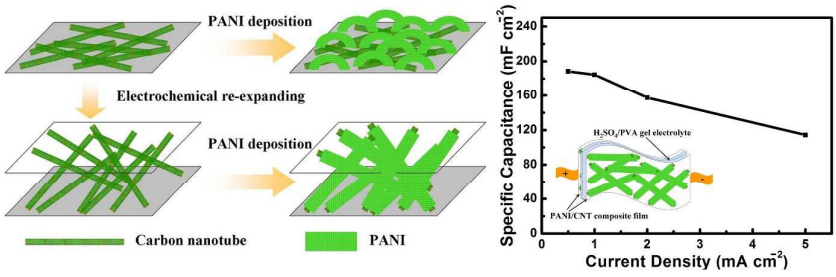

CNT film prepared via floating catalyst CVD method was activated by electrochemical strategy for better PANI growth. Both of this CNT/PANI hydrogel film electrode and flexible symmetric supercapacitor based on this electrode material exhibited high areal capacitance.